Formation and Evolution of Distorted Tulip Flames

Huahua Xiao[1, 2], Ryan W. Houim[1], Elaine S. Oran[1], and Jinhua Sun[2]
[1] University of Maryland
College Park, Maryland, 20742, USA
[2] University of Science and Technology of China
Hefei, Anhui Province, 230026, P.R. China

1 Introduction

A *tulip flame* is a laminar flame that develops a tulip-like shape as it propagates in a closed tube [1-4]. The initial flame may be convex, due to the confinement of the tube and interaction with boundary layers ahead of the flame, and this shape may eventually invert to become a concave propagating tulip flame. Tulip flames were first observed by photographs [5] showing that a tulip can develop in a closed tube when the aspect ratio of the tube is greater than two. After a tulip flame forms, it usually propagates down the tube until combustion is complete. In very long tubes, e.g., tubes with aspect ratio larger than 20, tulip flames collapse at some point and become convex toward the unburned mixture, and finally again develop a the tulip shapes [6]. To date, exactly how tulip flames form is not completely understood. Various elements of existing explanations include interactions of the flames with pressure waves [6], effects of viscosity and flame quenching [7, 8], hydrodynamic instabilities [2, 9], vortex structures forming in the burned gas [4], and Rayleigh-Taylor instabilities [1].

Recently, an additional complication was added with the discovery of the *distorted tulip flame* (DTF) [10-12]. These structures form after the usual tulip flame has formed, and they appear as additional cusps on the lips of the flame. Under some conditions, second DTF formed on the lips before the first DTF collapses [12].

What is missing from the discussion of both tulip flames and DTFs is an understanding of the interaction between the flame fronts and pressure waves generated by the flame as it propagates down the tube, and how this interaction might affect flame instabilities. Previous numerical studies [11, 13] could not resolve enough of the possible controlling phenomena because they used highly diffusive algorithms with inadequate numerical resolution. As a result, they could not provide enough detail to analyze the interactions among the flame front, pressure waves and boundary layers. Even the conditions required for a DTF to form are not well enough defined.

The work described here represents the first results of a study of the behavior and characteristics of DTF propagation using unsteady fully compressible computational fluid dynamics with high-order algorithms and adaptive mesh refinement (AMR). The goal is to produce an accurate calculation with a fine enough numerical mesh to resolve pressure waves and their interactions with flames and boundary layers, and then to compare these to prior experiments.

Correspondence to: Huahua Xiao, hhxiao@umd.edu

2 Prior Experiments

In the prior experiments [11, 12], the combustion chamber was a 53 cm long closed rectangular tube with a cross-section of 8.2 cm ×8.2 cm. The tube was filled with premixed stoichiometric hydrogen in air and ignited with a single spark gap near the left end wall on the tube axis. The evolution of the flame front was recorded with high-speed schlieren cinematography. Figure 2a, which shows the development of the tulip flame and the DTF, is taken from these experiments.

3 Physical and Numerical Models

The numerical simulations solve the two-dimensional (2D) fully compressible Navier-Stokes equations with a model of chemically reacting stoichiometric mixture of hydrogen and air. Details of the governing equations are in [14, 15]. The combustion of premixed stoichiometric hydrogen and air at 1 atm and 298 K is modeled by a single-step reaction [16]. The reaction rate is defined as $\Omega = A\rho Y \exp(-E_a / RT)$, where A, ρ , Y, R and E_a are the pre-exponential factor, density, unburned mass fraction, universal gas constant, and activation energy, respectively.

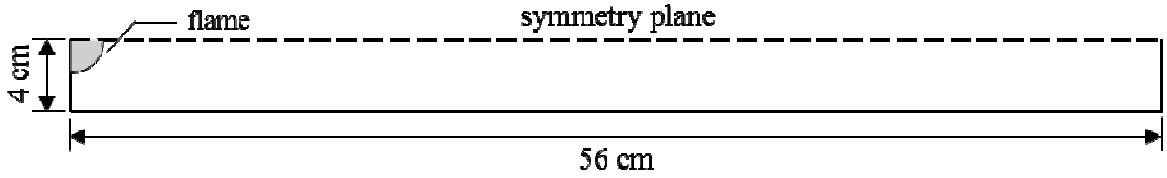

Figure 1. Computational domain. Walls are adiabatic with no-slip reflecting boundaries.

The equations are solved using a fifth-order MUSCL algorithm [17] with HLLC fluxes [18, 19]. Figure 1 shows the 2D computational domain, which describes an 8 cm × 56 cm channel. (Note that the geometry of the combustion chamber in the simulation is *slightly* different from that in the experiment.) AMR using the Paramesh library [20] provides local mesh refinement in the region of important features of the flow and combustion, such as flame fronts, strong pressure waves, and boundary layers. The minimum grid size is 15.625 μm, corresponding to 22 computational cells in the flame itself at initial conditions. The flame was ignited with a small circular pocket of hot, burned gas at the left end on the tube axis.

4 Flame Evolution in the Experiment and Numerical Calculation

Figure 2 shows the changes in flame shape as a function of time in (a) the experiment [12] and (b) the simulation. Both the experiment and the simulation show that the flame undergoes a series of shape variations, including a convex flame, flame inversion from convex to concave shape, tulip flames and DTF. The DTF develops into a triple tulip flame as secondary cusps approach the center of the primary tulip lips, e.g., at 7.8 ms in Fig. 2a. A second DTF is generated with a cascade of distortions superimposed on the primary lips, such as the flame at 9.0 ms in Fig. 2a, before the disappearance of the initials distortions.

The key features of flame-front evolution in the experiment are reproduced in the numerical simulation. In particular, the shape of the calculated DTF is close to the experimental observations. Compared to the previous numerical simulations [11, 13] in which the flame front was modeled on a very coarse grid, the present calculation provides a much more accurate representation. This will allow us to gain a deeper insight into the physical process and mechanisms controlling the flame evolution and perhaps some indication how the DTF arises.

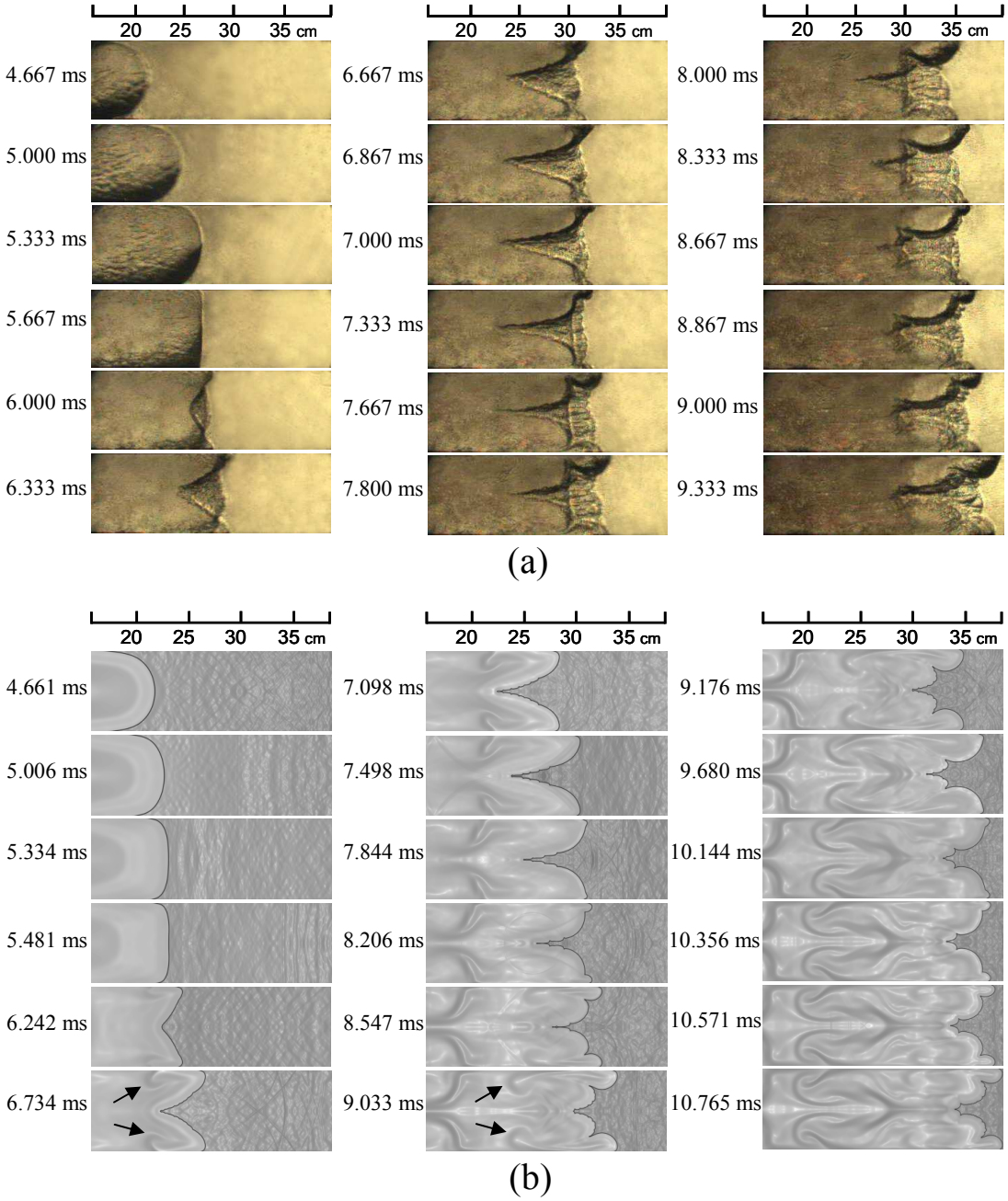

Figure 2. Sequences of premixed hydrogen/air flame front in (a) the experiment [12] and (b) the simulation. Note that the whole domain is not shown in the vertical direction in the experiment since both the schlieren upper and lower edges are 0.133 cm away from the lower and upper tube walls. The numerical schlieren images are shown for the same proportion. The heights of the domains shown in the images in the experiment and numerical simulation are 7.93 and 7.74 cm, respectively.

The dark spots (indicated by arrows in Fig. 2b at 6.734 ms) behind the tulip flame in the numerical simulation are the result of vortices in the burned gas which are created when the tulip flame is generated. These are also seen in the experiments of classical tulip flame by Dunn-Rankin and Sawyer [21, 22]. In the simulation, the vortex motion can also be observed as the distorted tulip flame forms, as shown at 8.547 and 9.033 ms (indicated by arrows as well) in Fig. 2b.

Figure 3 presents the position and propagation speed of (a) leading flame tip and (b) flame front along the centerline of the tube as a function of time. The flame oscillates until the end of the combustion process. When the flame touches the sidewalls or the flame cusp suddenly collapses, e.g., flames at 8.547 and 9.033 ms in Fig. 2b, additional pressure waves are generated. We have shown that these are expansion waves, and their presence causes the flame to oscillate. The collapsing flame cusp leads to a sudden increase of flame displacement speed along the tube centerline, as shown in Fig. 3b. This result explains the experimental observation of the steep increase of the primary tulip cusp speed in the previous work [11].

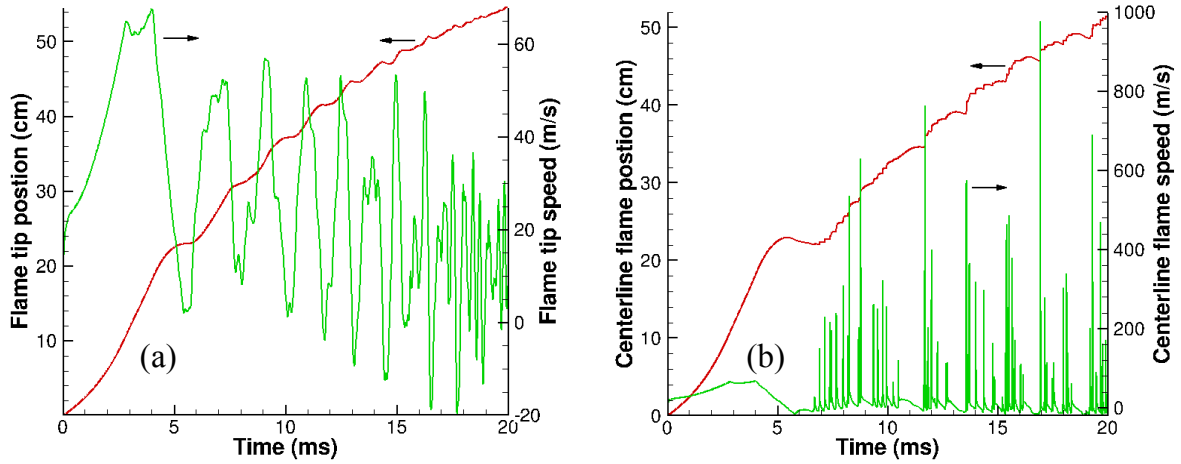

Figure 3. Time history of location and displacement speed of (a) the leading flame tip and (b) the flame front along the centerline.

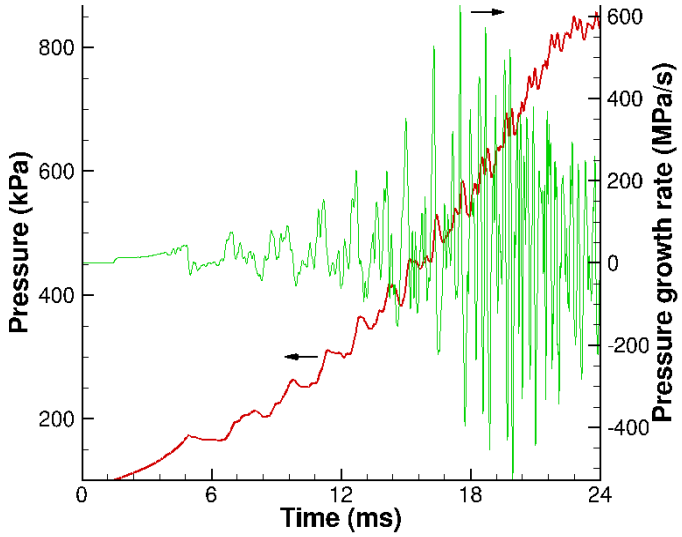

Figure 4. Pressure rise and pressure growth rate at the tube right end on the axis

Figure 4 shows the pressure and pressure growth rate as a function of time recorded at the right end wall of the tube on the axis. The pressure rise and growth rate also show oscillating behavior that is another indication of strong coupling of flame with pressure waves. The amplitude of the pressure oscillation increases very quickly when the flame approaches the right end. This implies that pressure waves are significantly amplified at the later stages of the burning process.

5 Discussion

The computation described here is only one of a series that we have performed to try to understand the development of the tulip flame and the unusual development of a distorted tulip flame. The entire series consists of variations in the aspect ratio and sizes of the tube, where the largest tube is 8 cm × 56 cm and the smallest is 1 cm by 7 cm. The experiments, described in prior papers [11, 12], were for the same mixture in a tube with the size 8.2 cm × 53 cm.

Even though we (and others) might postulate various mechanisms for the development of the first tulip flame [1, 3, 4, 6-8, 11, 23, 24], it is extremely difficult to understand why the subsequent DTF and succeeding shapes develop. Of particular interest is the second set of cusps, and why and how this forms is unclear at this stage.

The computations do, however, show that that pressure waves are extremely important. The movies (not shown in this abstract) of the schlieren images show pressure waves interacting and focusing, both in the burned and unburned regions, as the flame propagates down the tube. In addition, from a combination of our prior work and these computations, we believe that the presence of and changes in boundary layers and vorticity, all interacting with acoustic waves, is important and likely key to understanding the flame evolution. These will be shown and discussed in the presentation.

Acknowledgments

This work was supported by the University of Maryland through Minta Martin Endowment Funds in the Department of Aerospace Engineering, and through the Glenn L. Martin Institute Chaired Professorship at the A. James Clark School of Engineering. The authors also thank the support provided by National Natural Science Foundation of China (Projects Nos. 51406191 and 51376174) and the Chinese Postdoctoral International Exchange Program (2013).

References

[1] Clanet C, Searby G. (1996). On the "tulip flame" phenomenon. Combust. Flame. 105: 225.

[2] Dold JW, Joulin G. (1995). An evolution equation modeling inversion of tulip flames. Combust. Flame. 100: 450.

[3] Dunn-Rankin D, et al. (1986). Numerical and experimental study of "tulip" flame formation in a closed vessel. Proc. Combust. Inst. 21: 1291.

[4] Matalon M, Metzener P. (1997). The propagation of premixed flames in closed tubes. J. Fluid Mech. 336: 331.

[5] Ellis OCdeC. (1928). Flame movement in gaseous explosive mixtures. Fuel Sci. 7: 502.

[6] Guenoche H (1964) . Flame propagation in tubes and in closed vessels. In G. H. Markstein, (Ed.), Nonsteady Flame Propagation (pp. 107). New York: Pergamon Press.

[7] Marra FS, Continillo G. (1996). Numerical study of premixed laminar flame propagation in a closed tube with a full Navier-Stokes approach. Proc. Combust. Inst. 26: 907.

[8] Starke R, Roth P. (1986). An experimental investigation of flame behavior during cylindrical vessel explosions. Combust. Flame. 66: 249.

[9] Matalon M, Mcgreevy JL. (1994). The initial development of a tulip flame. Proc. Combust. Inst.: 1407.

[10] Xiao H, et al. (2011). Experimental study on the behaviors and shape changes of premixed hydrogen-air flames propagating in horizontal duct. Int. J. Hydrogen. Energ. 36: 6325.

[11] Xiao H, et al. (2012). Experimental and numerical investigation of premixed flame propagation with distorted tulip shape in a closed duct. Combust. Flame. 159: 1523.

[12] Xiao H, et al. (2013). An experimental study of distorted tulip flame formation in a closed duct. Combust. Flame. 160: 1725.

[13] Xiao H, et al. (2013). Dynamics of premixed hydrogen/air flame in a closed combustion vessel. Int. J. Hydrogen Energy. 38: 12856.

[14] Kessler DA, et al. (2010). Simulations of flame acceleration and deflagration-to-detonation transitions in methane - air systems. Combust. Flame. 157: 2063.

[15] Houim RW, Kuo KK. (2011). A low-dissipation and time-accurate method for compressible multi-component flow with variable specific heat ratios. J. Comput. Phys. 230: 8527.

[16] Gamezo VN, et al. (2008). Flame acceleration and DDT in channels with obstacles: Effect of obstacle spacing. Combust. Flame. 155: 302.

[17] Thornber B, et al. (2008). An improved reconstruction method for compressible flows with low Mach number features. Journal of Computational Physics. 227: 4873.

[18] Harten A, et al. (1983). On upstream differencing and Godunov-type schemes for hyperbolic conservation laws. SIAM Rev. 25: 35.

[19] Toro EF, et al. (1994). Restoration of the contact surface in the HLL-Riemann solver. Shock Waves. 4: 25.

[20] MacNeice P, et al. (2000). PARAMESH: A parallel adaptive mesh refinement community toolkit. Comput. Phys. Commun. 126: 330.

[21] Dunn-Rankin D, Sawyer RE (1985). Interaction of a laminar flame with its self-generated flow during constant volume combustion. 10th ICDERS. Berkley, California: 115

[22] Dunn-Rankin D, Sawyer RF. (1998). Tulip flames: changes in shape of premixed flames propagating in closed tubes. Exp. Fluids. 24: 130.

[23] Rotman DA, Oppenheim AK. (1986). Aerothermodynamic properties of stretched flames in enclosures. Proc. Combust. Inst.: 1303.

[24] Metzener P, Matalon M. (2001). Premixed flames in closed cylindrical tubes. Combust. Theor. Model. 5: 463.